Available online at www.sciencedirect.com
SCIENCE DIRECT®
Spectrochimica Acta Part B 58 (2003) 1375–1389
SPECTROCHIMICA ACTA PART B
www.elsevier.com/locate/sab

Development of a direct hydride generation nebulizer for the determination of selenium by inductively coupled plasma optical emission spectrometry☆

Nereida Carrión[a,*], Miguel Murillo[a], Edie Montiel[b], Dorfe Díaz[a]

[a]*Centro de Química Analítica, Escuela de Química, Universidad Central de Venezuela, Apartado de Correos 47102, Caracas 1041A, Venezuela*
[b]*Instituto de Zoología Tropical. Facultad de Ciencias, Universidad Central de Venezuela, Apartado de Correos 47102, Caracas 1041A, Venezuela*

Received 28 August 2002; accepted 14 April 2003

Abstract

A study was conducted to evaluate the performance of a new direct hydride generation nebulizer system for determination of hydride forming elements by inductively coupled plasma optical emission spectroscopy. This system was designed and optimized to obtain the highest sensitivity. Several experimental designs were used for these purposes. To optimize the individual parameters of the system, and to study the interaction between these parameters for both direct hydride generation nebulizers, a central composite orthogonal design with eight factors was set up. Significant behavioral differences were observed in the two direct hydride generation nebulizers studied. Finally, a 70 μm gas orifice nebulizer exhibits a better detection limit than the 120 μm nebulizer. Generally, for determination of selenium, this new direct hydride generation nebulizer system exhibits a linear dynamic range and detection limit (3σb) of 3 orders of magnitude and 0.2 μg l^{-1} for selenium, respectively. This new hydride generator is much simpler system that conventional hydride generation systems, which does not need to be changed to work in normal mode with the inductively coupled plasma, since this system may be used for hydride forming elements and those that do not form them. It produces a rapid response with low memory effect. It reduces the interference level of Ni, Co and Cu to 600, 500 and 5 mg l^{-1}, respectively. The accuracy of the system was verified by the determination of selenium in several standard reference materials of ambient, food and clinical sample matrices. No statistically significant differences (95 confidence level) were obtained between our method and the reference values.

Keywords: Hydride generation; Hydride generation-inductively coupled plasma optical emission spectrometry (HG-ICP-OES); Selenium determination; Experimental design; Orthogonal design; Response surface methodology

☆ This paper was presented at Federation of Analytical Chemistry and Spectroscopy Societies Annual Meeting, held in Detroit, USA, October 2001.

*Corresponding author. Fax: +58-212-693-4977.
E-mail address: ncarrion@strix.ciens.ucv.ve (N. Carrión).

0584-8547/03/$ - see front matter © 2003 Elsevier Science B.V. All rights reserved.
doi:10.1016/S0584-8547(03)00078-8

1. Introduction

Selenium is an essential element in the development of organisms. At low concentrations, anomalies are observed due to specific biochemical changes [1,2]. However, at higher concentrations it becomes a toxic element [3]. This dual behavior of selenium has stimulated the development of numerous methods for its determination in environmental and biological samples [4]. Normally, selenium is found in very low concentrations for its determination by inductively coupled plasma optical emission spectrometry (ICP–OES) with the conventional methods of nebulization of liquid samples. Nevertheless, with a Hydride generation (HG) procedure, better sensitivity is achieved in one or two orders of magnitude with respect to the sample solution nebulization techniques. This is mainly due to the high efficiency of analyte transport; atomization and excitation of the hydride in the ICP source [5], and at the same time the mutual interferences from hydride-forming elements are absent [6]. One of the main inconveniences in HG by reduction with sodium tetrahydroborate ($NaBH_4$) in acid medium is the interferences produced by the transition metals [5–10]. It has been reported that these elements interfere in the hydride formation process after being reduced to metals or after being converted to metal borides [5,11,12]. The catalytic effect of the colloidal metals on decomposition of tetrahydroborate [13] or the transport to the atom cell [14] or to ICP [15] during a hydride generation process has also been considered to be another source of interference. Lugowska and Brindle [16] have studied the mechanisms of interference of nickel, iron and cobalt in the suppression of the selenium hydride signal in hydride generation. They found that the $NaBH_4$ reaction prevails with the interfering metal in comparison with its reaction with H^+. They also proved the formation of boride-like species. Both lead to inhibiting the formation or decomposition of the hydride once formed. Transport of transition metals to the ICP during a hydride generation process has also been studied. The amount of metals transferred into the plasma increases when the concentration of $NaBH_4$ and acid is increased [14,15]. The magnitude of the interference depends on the acid concentration of the reaction medium [10,15], reductant concentration [14] and the hydride generator systems used to produce and transport the gaseous hydride to the ICP source. The design of the HG device is decisive in the time of contact between the formed hydride and the sample matrix [17,18].

Thompson et al. [19] were the first to use HG as a procedure for introduction of the sample into an ICP for the simultaneous determination of As, Sb, Bi, Se and Te. The best LODs were found with a high power ICP and with 5 M HCl. They found LODs 500 times lower with respect to pneumatic nebulization. Goulden et al. [20] used a low power plasma (power of 1400 W) for As and Se determination and a torch of larger diameter than usual, which provides stability to the plasma discharge. Hwang et al. [21] described a simple continuous flow mode HG system for a 1-kW ICP–OES. The sample and reductant were continuously pumped into the hydride generator and the waste sample was continuously removed to ensure a constant pressure. Brindle et al. [22] reported a generator-separator, in which hydride formation takes place at the outlet of the two capillaries that transport the sample and the $NaBH_4$, respectively. This HG system was used with direct current plasma (DCP) [22] or in an ICP [23] for Se determination. Another form of generating the hydride in a continuous manner is hydride generation using a modified nebulizer device, [17,18,24–27], in which the sample and the reducing agent supply is integrated to the nebulizer, thus resulting in the reaction being performed within the aerosol, on contact with the small droplets of sample and reductant. Wolnik et al. [24] described a tandem nebulization system that makes it possible to carry out a simultaneous analysis of volatile elemental hydrides as well as other elements. With this system, the LOD is improved by 6 to 40 times for the hydride-forming elements without decreasing the sensitivity for those that do not form it. Huang et al. [25] developed a nebulizer-hydride generator system in which large droplets of the acid sample aerosol from the pneumatic nebulizer were trapped by the impact wall of a smoking-pipe shaped HG, and reacted with reductant. The

LOD for the hydride-forming element could be improved over 20 times compared to that obtained with the conventional nebulizer. The LODs of other elements remained unaffected. Feng et al. [26] designed a small concentric HG without gas–liquid separator, which was used with a 0.65 kW mini-torch for As determination. The Sturgeon group [17,18] studied a new hydride generator system based on the insertion of a capillary tube into the sample introduction channel of a standard nebulizer. In the first design, this device terminates in a 1.5 cm chamber from the end of nebulizer orifice [17] and they used a gas–liquid membrane separator. With this system they managed to increase the tolerance limits of transition elements without interference in selenium determination to very high values. The LOD obtained by ICP–OES was 6 $\mu g\ l^{-1}$. This LOD was improved 3 times with a new design in which the chamber is eliminated [18] at the nebulizer outlet and the gas–liquid separator. This was replaced with a conventional Scott double-pass spray chamber. Although they achieved extremely high tolerance levels for the transition metals for selenium hydride generation, the LOD decreased by one order of magnitude with respect to conventional HG techniques [7–9,19–21] and those of the same gender [24]. This same principle was used to modifier a commercial Gem Tip™ cross-flow nebulizer. A narrow Teflon™ tube was inserted into to nebulizer tip through the Teflon™ sample introduction tube. It was used for ICP–MS [27] obtained an enhanced sensitivity and low background from aerosol transport with this system.

When the effect of a variable is not independent from the others, as usually occurs in chemistry, the use of statistical uni-factorial techniques can lead to erroneous conclusions [28]. In these cases, it is advisable to use factorial designs that permit useful information to be obtained from the main effects such as their interaction. Chemometric methods are increasingly used in the optimization of analytical systems such as hydride generation atomic spectrometric techniques [29,30]. The main objective of the response surface methodology is to determine the optimal operational conditions of the system; this has been widely used in the optimization of processes [31], optimization of analytical methods [29,32] and sample treatments [33].

The aim of this study was to evaluate the performance of a new hydride generator for hydride forming elements for determination by inductively coupled optical emission spectroscopy taking into account the advantages of nebulizer-hydride generator systems as sample introduction devices for the ICP. In order to consider the effects of all possible variables that affect the sensitivity, experimental design, such as the central composite orthogonal design has been used throughout the optimization. The optimum values of the parameters for selenium determination were calculated using this approach.

2. Experimental

2.1. Instrumentation

Measurements were performed with a Jobin Yvon sequential ICP spectrometer Model JY-24, operated under the conditions shown in Table 1. The original gas flow meters for the aerosol carrier were replaced by mass flow controllers (Brooks 5850E). A quartz torch and alumina injector tubes were used.

A hydride generation system to obtain the highest sensitivity was designed and optimized. For this propose, a V-groove Babington-type nebulizer having two solution channels was designed and constructed in our laboratory. Fig. 1 shows a schematic diagram of the new direct hydride generation nebulizer system (DHGN). The design of the first (Fig. 1a) was based on a V-groove Babington-type nebulizer constructed with a 120 μm gas orifice and two solution input channels. These channels were used for delivery of the tetrahydroborate solution and sample solution, respectively. The second system (Fig. 1b) was based on a V-groove Babington-type nebulizer with a 70 μm gas orifice, which was modified by adding a second solution input channel for delivery of the tetrahydroborate solution. These systems were coupled with a conventional Scott double pass spray chamber. For the optimization studies two peristaltic pumps Pharmacia model Peristaltic Pump P-1.d were used to deliver both the sample

Table 1
Optimal working conditions for ICP–OES system

Rf power	1.3 kW
Frequency of RF generator	40 MHz
Outer gas flow rate	18 l min^{-1}
Observation height	15 mm (above load coil)
Analytical line: Se(I)	196.03 nm
Carrier gas flow rate	500 ml min^{-1}
Hydride Generator	
Sample flow rate	1 ml min^{-1}
Sample solution acidity	2.3 M HCl
$NaBH_4$ solution flow rate	0.7 ml min^{-1}
$NaBH_4$ concentration (in 0.05% m/v NaOH)	0.3% (m/v)

and $NaBH_4$ to the nebulizer. Two pumps were necessary and were able to cover the wide variety of flow rates required in the statistical optimization. For the analytical measurement, a four-channel peristaltic pump Gilson model Minipulse was used for both the sample and $NaBH_4$ to delivery to nebulizer.

A CEM model MDS-2000 microwave digester was used for closed vessel high-pressure sample dissolution.

2.2. Reagents

All chemicals used were of analytical-reagent grade. Distilled, de-ionized water (DDW) was

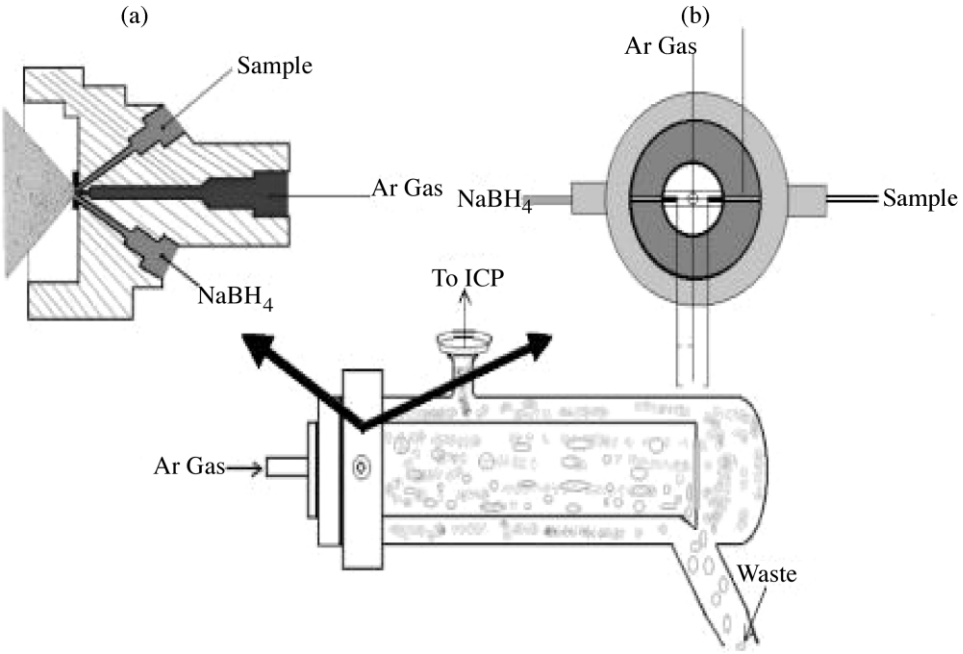

Fig. 1. Schematic of the nebulizers. (a) 120 μm, (b) 70 μm.

obtained from a Barnstead Nanopure system. HCl (Merck), HNO_3, H_2O_2, HF (Riedel de Haën), H_3BO_3 and H_2SO_4 (Baker Analized) were used without further treatment. For interference studies, 1000 μg/ml Cu, Co and Ni standard solutions (Riedel de Haën) were used. A 10 μg ml^{-1} stock solution of Se(IV) was prepared by the following procedure: 1 ml of 1000 μg ml^{-1} in HNO_3 (Fischer Scientific) 2% (m/v) adding 1 ml of 18 M H_2SO_4 and 10 ml of 4 M HCl, were heated in a water bath until elimination of the murky vapors was achieved, then the solution was diluted to 100 ml with 4 M HCl in a volumetric flask. Low concentration standards required for response curves were prepared by serial dilution with dilute acid as required. All standards were prepared in the same way as the samples. The Se(VI) was reduced to Se(IV) in 4 M HCl by heating at 90 °C for 30 min. Solutions of $NaBH_4$ (Alfa Chemicals Inc) were prepared daily at a concentration of 0.3% (m/v) in 0.05% (m/v) NaOH (Fisher Scientific).

2.3. Reference materials

Validation of the method described in this work was performed using several certified reference materials, which were chosen to represent food and clinical sample matrices: not-fat milk powder (NIST 1549), oyster tissue (NIST 1566a) and human urine (Urine metals control Lyphochek®). The reference materials sediment (IAEA/soil-7) was also analyzed.

2.4. Reference material treatment

Prior to analysis, the human urine reference material was reconstituted as recommended by the supplier. Decomposition of the other reference materials was carried out by microwave assisted acid attack. The sediment (IAEA/soil-7) standard reference material was digested following the EPA 3052 procedure for digestion of siliceous and organic based matrices [34]. A 0.2000 g subsample of sediment was placed in the 30-ml Teflon™ vessel of the microwave digestion system, and 3 ml of concentrated HNO_3, 1 ml of concentrated HF and 2 ml of 30% (m/v) H_2O_2 were added. The vessel were sealed and heated in the microwave oven under the following conditions: 40 min at pressure of 140 psi and 50% power. After cooling, 7 ml of 5% (m/v) H_3BO_3 solution were added, and finally the solution was diluted to 50 ml using 2 M HCl.

Not-fat milk powder (0.5000 g) and oyster tissue (0.1000 g) were treated as follows. The sample was weighed into the 30-ml Teflon™ vessel of the microwave digestion system; 3 ml of concentrated HNO_3 and 1 ml of water were added and the closed sample heated following the temperature program recommended by the supplier [35]. The solution was made up to 50 ml using 2 M HCl.

One ml of human urine (Urine metals control Lyphochek®) was digested with a mixture of HNO_3–H_2SO_4 (2:1) (2 ml) for 30 min in an ultrasonic bath, and the resulting solution made up to 10 ml with 2 M HCl.

All samples were subjected to the same procedures for elimination of HNO_3 and reduction of Se(IV).

2.5. Measurement

The acidified samples and reductant were simultaneously pumped into the hydride generator system. In the region of convergence of the two solutions and the carrier gas, sample and $NaBH_4$ aerosol was generated and a reaction occurred to produce the selenium hydride and hydrogen. One minute was needed to reach the stable steady-state signal.

2.6. Design and analysis of experiments

A two level full factorial design was applied to determine the magnitude of the main variables and their interactions. The values of the variables for each level were 0.50 and 0.30 l min^{-1} for carrier gas flow rate (A), 4 and 2 mol l^{-1} for the sample acid concentration (B), 1.2 and 0.6 ml min^{-1} for sample solution flow rate (C), 0.6 and 0.2% w/v for $NaBH_4$ concentration (D) and 0.8 and 0.2 ml min^{-1} for $NaBH_4$ solution flow rate (E). A central composite orthogonal design with eight factors was used with two dependent variables: the nebu-

Table 2
Factors and levels used in the experimental design

Factors	Levels				
	Axial-α (−2.828)	Low (−1)	Central (0)	High (+1)	Axial + α (+2.828)
A–carrier gas flow rate (l min^{-1})	0.213	0.35	0.43	0.50	0.640
B–Acid concentration (mol l^{-1})	1.689	2.00	2.17	2.34	2.651
C–Sample flow (ml min^{-1})	0.13	1.5	2.25	3.0	4.37
D–$NaBH_4$ concentration (% m/v)	0.0130	0.15	0.23	0.3	0.44
E–$NaBH_4$ flow (ml min^{-1})	0.009	1.0	1.5	2.0	2.0
F–Ni concentration (mg l^{-1})	10.0	100.0	150.0	200.0	240.0
G–Co concentration (mg l^{-1})	12.0	30.0	40.0	50.0	70.0
H–Cu concentration (mg l^{-1})	0.4	5.0	8.0	10.0	15.0

lizers: 70 and 120 μm to optimize the respective response. The independent variables mentioned above were employed. In addition, a study of some potential interference such as Cu, Co and Ni was included. The emission signal intensity was used as the dependent variable. Optimization was accomplished by using a solution containing 100 μg l^{-1} of Se. The experimental design requires 90 experiments performed in 5 blocks of 18 experiments each. Estimation of the parameters of the models and their significance were evaluated applying an ANOVA procedure. The statistical designs were created and analyzed with Design Expert 6.0.4 (2001) = [36], JMP 3.2.1 (1997) [37] and Mathematica 2.1 (1996) software package [38]. Table 2 shows the real, coded factors and levels used in the experimental design.

3. Results and discussion

3.1. Study of significant factors

The emission signal for selenium hydride is considered to be a function of several variables. In order to identify the significant factors, a two-level factorial design was applied to study plasma conditions for both nebulizers. The results of this study showed that the lineal terms have significant effects and that several interaction and quadratic terms were significant. Likewise, significant effects were different for both nebulizers. This result seems logical since the diameter of the gas outlet of the cross-flow nebulizers regulates the gas exit pressure and, therefore, the droplet diameter and droplet density of primary aerosol [39]. These parameters affect the droplet collisions between reductant and sample, where the reduction reaction takes place to generate the selenium hydride. This parameter also affects the transport of the analyte to the ICP.

3.2. Optimization of the experimental conditions

The optimal conditions for the two-design direct hydride generation nebulizer system (DHGN) were studied. Since interactions exist between the factors, the use of uni-factor statistical techniques to optimize the experimental conditions as usual does not provide the best results. Therefore, a multi-factor experimental design was applied in order to obtain useful information, not only of the main effects, but also the interaction of two or more factors. Owing to the fact that one of the main inconveniences in GH with reduction by $NaBH_4$ in an acid medium are the interferences, due to the ions of the transition metals [5–10,13,16–18], Ni, Co and Cu were included as variables in the optimization study. The primary objective in obtaining a response surface is to aid the statistician and other statistics users in applying the response surface procedure to appropriate problems in many fields. The type of problems in which the Response of surface methodology (RMS) is most effectively used when the experimenter is interested in finding a suitable approximating function to predict future response, as well

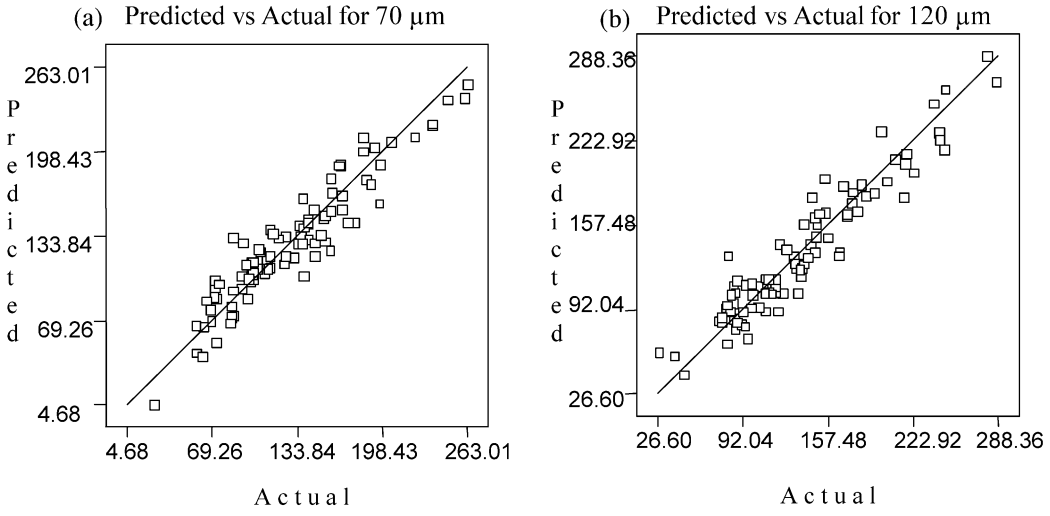

Fig. 2. Fit of data to the estimated equation. (a) 70 μm nebulizer and (b) 120 μm nebulizer.

as to determine the optimum value of the independent variable, as far as response is concerned. Two central composite orthogonal designs with eight independent variables and two dependent variables were used. The independent variables were carrier gas flow rate, acid concentration of the sample, sample solution flow rate, $NaBH_4$ concentration, $NaBH_4$ solution flow rate, Ni concentration, Co concentration and Cu concentration. The dependent variables were the 70 and 120 μm DHGNs.

The canonical equations for each of the dependent variables obtained are:

(70 μm DHGN):

$$\overline{Y}_1 = 110{,}25 - 1.117W_1^2 - .25W_1 + 5.069W_3^2 + .46W_4^2 - 3.96W_5^2 - 1.962W_6^2 - 3.43W_7^2 - 1.01W_8^2$$

(120 μm DHGN):

$$\overline{Y}_2 = 57.79 - 9.83W_1^2 + 8.26W_1 + 4.50W_3^2 + 1.91W_4^2 + 1.69W_5^2 - .39W_6^2 - 3.53W_7^2 - 7.99W_8^2$$

where W_1 is carrier gas flow rate (A), W_2 is acid concentration sample (B), W_3 is sample solution flow rate (C), W_4 is $NaBH_4$ concentration (D), W_5 is $NaBH_4$ solution flow rate (E), W_6 is Ni concentration (F), W_7 is Co concentration (G) and W_8 is Cu concentration (H).

At the stationary point, the surfaces are the saddle point in the fitted surface for both cases. The critical values are outside the range.

Fig. 2 shows the chart of the data adjustment to the estimated equation for both DHGNs. In both cases, a homogenous dispersion of the points at approximately 45° straight line is observed, thus corroborating the multiple regression equations obtained are well adjusted to the experimental values. The 70 μm DHGN (Fig. 2a) is better adjusted to the model as the points are less dispersed.

The analysis of variance (ANOVA) of the model is shown in Table 3 and Table 4. Analysis of the result showed that linear interactions and quadratic terms have significant effects ($P<0.05$). The behavior of the two nebulizers is different. The 70 μm DHGN is affected by a greater number of factors than the 120 μm DHGN. Carrier gas flow rate, sample solution flow rate, $NaBH_4$ concentration, Cu concentration show a significant effect for both DHGN, while $NaBH_4$ solution flow rate is only significant for the 70 μm DHGN. The Ni concentration is only significant for the 120 μm DHGN.

The interaction between $NaBH_4$ concentration and $NaBH_4$ solution flow rate (DE) shows a significant effect for both nebulizers. For the 70

Table 3
70 μm nebulizer. ANOVA for response surface quadratic model analysis of variance (Partial sum of squares)

Source	Sum of squares	DF	Mean square	*F* value	Prob > *F*
Block	17284.36	4	4321.09		
Model	1.804E+005	44	4099.66	6.47	<0.0001*
A: carrier gas flow rate	19331.20	1	19331.20	30.49	<0.0001*
B: acid concentration	2198.00	1	2198.00	3.47	0.0698
C: sample flow rate	53310.12	1	53310.12	84.09	<0.0001*
D: $NaBH_4$ concentration	21395.41	1	21395.41	33.75	<0.0001*
E: reductor flow rate	19675.46	1	19675.46	31.03	<0.0001*
F: Ni concentration	3.20	1	3.20	5.052E-003	0.9437
G: Co concentration	34.41	1	34.41	0.054	0.8169
H: Cu concentration	23828.64	1	23828.64	37.58	<0.0001*
D^2	8166.05	1	8166.05	12.88	0.0009*
H^2	3307.01	1	3307.01	5.22	0.0276*
CD	4314.85	1	4314.85	6.81	0.0126*
CE	6058.68	1	6058.68	9.56	0.0036*
CH	2967.53	1	2967.53	4.68	0.0364*
DE	3869.46	1	3869.46	6.10	0.0177*
Residual	25993.98	41	634.00		
Lack of fit	23655.32	36	657.09	1.40	0.3815
Pure error	2338.66	5	467.73		
Cor total	2.237E+005	89			

* Significant.

μm DHGN, the interaction between sample solutions flow rate and $NaBH_4$ concentration (CD), and sample solution flow rate and $NaBH_4$ solution flow rate (CE), are also significant. It is important to note that the interactions among factors showing a significant effect are actually the factors involved in the reduction reaction to form the selenium hydride.

Fig. 3 shows the perturbation plot. The perturbation plot provides a silhouette view of the response surface. The benefit obtained from this plot is the selective axis and constant contour

Table 4
120 μm nebulizer. ANOVA for Response Surface Quadratic Model Analysis of variance (Partial sum of squares)

Source	Sum of squares	DF	Mean square	*F* value	Prob > *F*
Block	18512.50	4	4628.12		
Model	2.214E+005	44	5032.84	7.89	<0.0001*
A: carrier gas flow rate	11683.54	1	11683.54	18.32	0.0001*
B: acid concentration	2487.48	1	2487.48	3.90	0.0551
C: sample flow rate	1.521E+005	1	1.521E+005	238.46	<0.0001*
D: $NaBH_4$ concentration	2644.63	1	2644.63	4.15	0.0482*
E: reductor flow rate	363.96	1	363.96	0.57	0.4544
F: Ni concentration	3155.20	1	3155.20	4.95	0.0317*
G: Co concentration	98.73	1	98.73	0.15	0.6961
H: Cu concentration	15996.01	1	15996.01	25.08	<0.0001*
C^2	6691.70	1	6691.70	10.49	0.0024*
DE	8250.77	1	8250.77	12.93	0.0009*
Residual	26154.77	41	637.92		
Lack of fit	21784.64	36	605.13	0.69	0.7678
Pure error	4370.13	5	874.03		

* Significant.

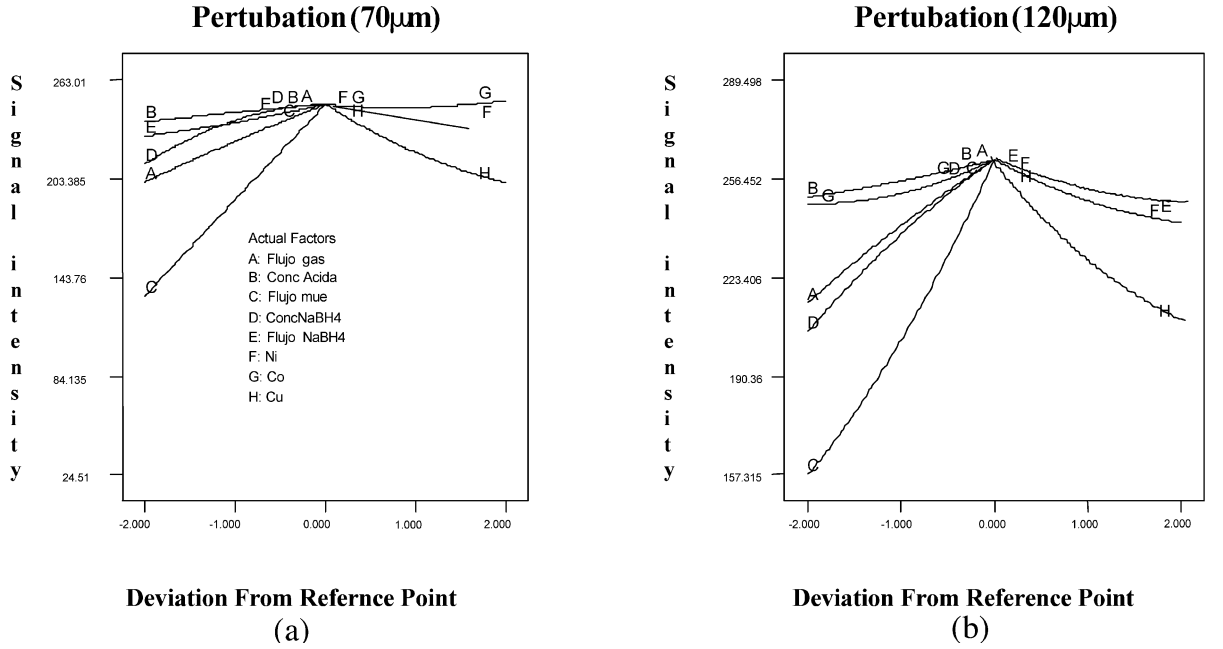

Fig. 3. Perturbation plots (a) 70 μm nebulizer and (b) 120 μm nebulizer.

provided by the 3D plot. For response surface designs, the perturbation plot shows the response changes as each factor moves from the chosen references point with all other factors held constant at the reference value [40]. In Fig. 3a, it is possible to see for the 70 μm DHGN, how the magnitude of the effect of the variables impact in the following order: the sample solution flow rate > Cu concentration > $NaBH_4$ concentration > $NaBH_4$ solution flow rate > carrier gas flow rate. For the 120 μm DHGN (Fig. 3b) these are sample solution flow rate > Cu concentration > carrier gas flow rate > Ni concentration. The response from acid concentration sample is invariant within this concentration range studied. This behavior was similar to that reported by Mianzhi and Barnes [7], Nakahara and Kikui [8] and Tao and Sturgeon [18], yet Thompson et al. [19], Ding and Sturgeon [17], Rigby and Brindle [23], find an increase of the signal with the increase of acidity of the sample reaching a plateau at concentrations of 3 M to 4.5 M HCl, respectively.

The program used also supplies information on each of the factors separately and provides the corresponding charts performed with five experimental points. The results of this study showed a greater influence of the variables on the emission signal in the 70 μm DHGN with respect to that of 120 μm DHGN. For both DHGNs, an increase in the carrier gas flow rate produces an enhancement of the emission signal in the range studied. The transport efficiency of the generated hydride to the ICP is enhanced as usual. The sample solution flow rate had a positive effect on the emission signal in the range studied. This effect was expected since an increase in the sample solution flow rate increased the amount of analyte reaching the plasma discharge. The $NaBH_4$ concentration was also a very important factor for both DHGNs with a positive effect on the selenium hydride production. An increase in $NaBH_4$ concentration increases the rate of the reaction and, therefore, the amount of hydrogen produced and this augments the transport efficiency. It was observed that for the 70 μm DHGN, this effect was greater (quadratic effect). Perhaps this is due to the fact that the 70 μm DHGN, the reduction reaction is more efficient as this nebulizer produces

an aerosol of smaller droplet diameter and greater droplet density of primary aerosol, thus propitiating a greater number of collisions between the sample and reductant solution.

For the 120 μm DHGN, the $NaBH_4$ solution flow rate is not a significant effect, while it is for that of 70 μm. With this nebulizer an increase in the emission signal with increase in the $NaBH_4$ solution flow rate was found as expected, since increase in the $NaBH_4$ solution flow rate augments the amount of reducing agent available for selenium hydride formation. Nevertheless, this effect is not observed in the 120 μm DHGN, perhaps because with this nebulizer an increase in flow of the reductant produces an increase in droplet density, and as these have larger droplet diameter, they tend to condense rapidly.

The Cu concentration had a negative effect on the Se emission signal. This depressive effect is more pronounced in the 70 μm DHGN than in the 120 μm DHGN. It may due to the fact that the 70 μm DHGN forms a finer and dense primary aerosol, thus favouring the reduction reaction of Cu^{+2} to Cu. Which interferes in the formation and/or the transport of the selenium hydride formed [10,15]. The Ni concentration had a slightly negative effect on the Se emission signal in the 120 μm DHGN.

The H_2Se formation reaction system occurs within the aerosol by collisions between droplets of the sample in an acid medium and the $NaBH_4$ droplets in a basic medium. Furthermore, this aerosol contains argon (carrier gas), H_2Se (gaseous), CO_2, H_2O and H_2 (gas). The dynamics of this system are linked to the phenomena of transport of the aerosol and gases present; in addition to the chemical and instrumental parameters which can influence both the formation of H_2Se and the physical conditions of the plasma. The graphic representation of the response surface is an approximation to help visualize these phenomena, since the tendency of each factor is not easy to imagine in an octagonal surface.

Fig. 4 shows the response for two factors, the concentration and flow solution rate of $NaBH_4$ in the 120 μm DHGN. By increasing the $NaBH_4$ concentration and decreasing the $NaBH_4$ flow, the signal increases slightly, as better seen in the

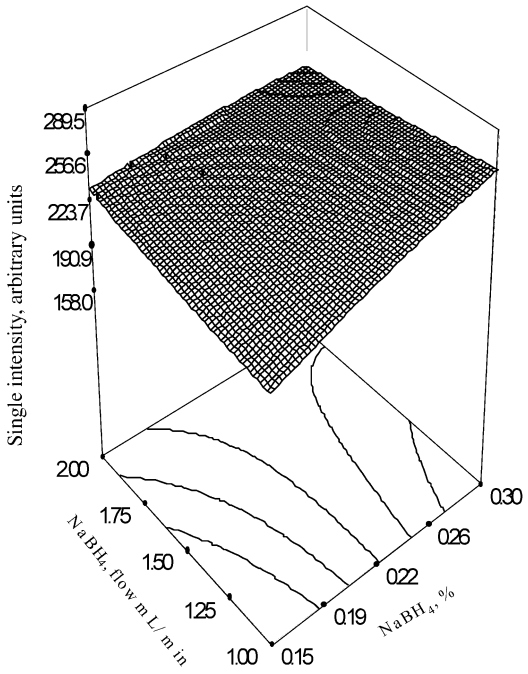

Fig. 4. Response surfaces estimated for the 120 μm nebulizer; $NaBH_4$ flow vs. $NaBH_4$ concentration.

contour surface zone where the beginning of an optimum is observed. Possibly, this slight increase in the emission signal of the selenium with an increase in the $NaBH_4$ concentration and a decrease in $NaBH_4$ flow is due to an increase of the amount of hydrogen generated. However, we do not necessarily have the same effect when the $NaBH_4$ flow is increased, since the acid concentration in the new drops formed for collisions between the sample and reductan solution decreases due to presence of NaOH solution (0.05% w/v).

The response surfaces for the significant interactions for the 70 μm DHGN are shown in Fig. 5. Fig. 5a shows the estimated response surface from central composite orthogonal design of the $NaBH_4$ concentration against the sample flow. Here, we are able to see that the signal reaches a maximum intensity, which remains constant while the sample flow and $NaBH_4$ concentration continue to increase. This occurs at 0.8 ml/min for sample delivery and 0.25% $NaBH_4$ concentration. Fig. 5b shows the response and sample flow contour sur-

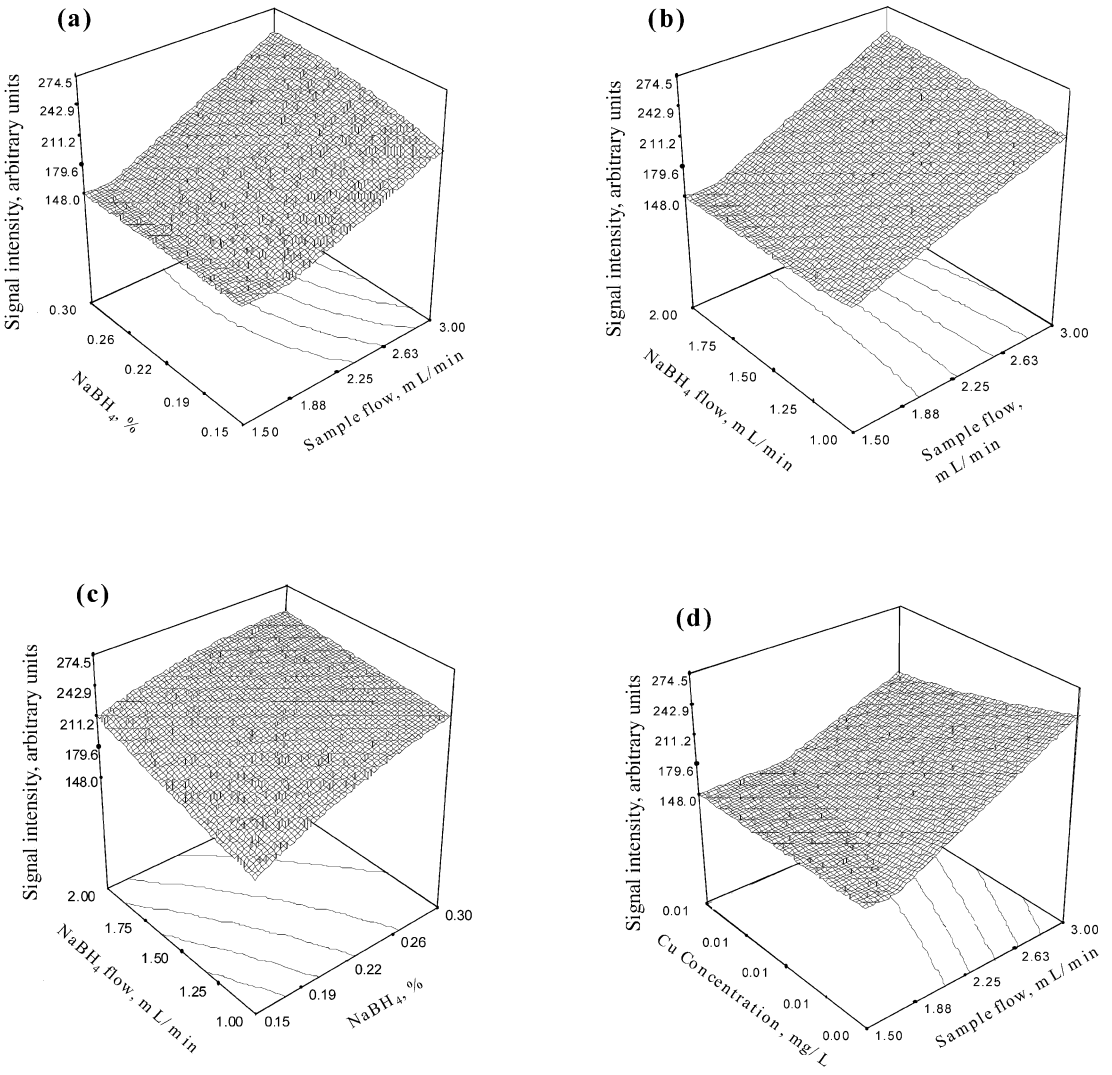

Fig. 5. Response surfaces estimated for the 70 μm nebulizer; (a) $NaBH_4$ concentration vs. sample flow. (b) $NaBH_4$ flow vs. sample flow. (c) $NaBH_4$ flow vs. $NaBH_4$ concentration and (d) Cu concentration vs. sample flow.

face against the $NaBH_4$ flow. The emission signal increases with increased sample and $NaBH_4$ flow rates. As in the above case, a point is reached where the signal remains constant. In both cases, possibly the excess of H_2 formed in the H^+ reaction with the $NaBH_4$ increases the injection flow and consequently decreases the residence time of the analyte in the ICP. In Fig. 5c, the $NaBH_4$ concentration response surface against $NaBH_4$ flow is represented. The surface remains close to optimum even when $NaBH_4$ concentration and $NaBH_4$ flow rate are increased. This appears intuitively correct, since the two factors together determine the total amount of $NaBH_4$ available for the hydride generation reaction. It is seen in the range studied that a maximum situation is still not reached. However, the optimum conditions may be calculated from the canonic equation representing the behavior of the variables. Fig. 5d shows the function for Cu concentration vs. sample flow

rate. The response is directly proportional to the sample solution flow rate and inversely proportional to Cu concentration. As Cu concentration is decreased, there is a zone where the signal is constant, since the interfering effect on the selenium signal is not produced from this concentration.

Optimal working conditions of maximum sensitivity found are the same for both DHGN, as shown in Table 1.

3.3. Figures of merit and characteristics of the system

Transition metals, such as Cu^{2+}, Ni^{2+} and Co^{2+}, interfere severely with the generation process [5], selenium being the most sensitive to this type of interferences [8]. The effects of the nickel, cobalt and copper on the selenium emission signal were, therefore, studied.

Copper produces the greatest effect on the signal. It has been reported [7] that the effect of Cu(II) on SeH_2 evolution in HG–ICP OES increased with higher Cu level and decreased with increasing Se level [7]. It is important to take this into account when comparing the results of the interference tolerance levels. Mianzhi and Barnes [7], using a batch system reported that at 1 mg l^{-1} of Cu the interfering effect is considerable for Se concentrations of 10 to 300 μg l^{-1} (interference/selenium ratio 10 to 3.3). Nakahara and Kikui [8] with a continuous flow system report this effect after 0.1 mg l^{-1} of Cu for 200 μg l^{-1} of Se (interference/selenium ratio 0.5). Stripeikis et al. [10] report that the signal from 20 μg l^{-1} Se remains constant up to 3 mg l^{-1} (interference/selenium ratio 150) in 7 M HCl and 0.1 mg l^{-1} (interference/selenium ratio 5). At 3.5 M HCl, Tao and Sturgeon [18] with a nebulizer-hydride generator report that 20 mg l^{-1} of Cu could be tolerated without affecting the signal from 500 μg l^{-1} of Se (interference/selenium ratio 40). In the nebulizer-hydride proposed generator, the emission signal from 20 μg l^{-1} of Se without masking reagent remained practically unaffected by the presence of up to 5 mg l^{-1} of Cu (the interference/selenium ratio 250).

The Ni(II) ions suppresses the H_2Se signal during hydride generation. The mechanisms whereby this interference is produced have been studied by Lugowska and Brindle [17], who found that the $NaBH_4$ reaction prevails with the metal and presence of boride-like species, thus suggesting that hydride is neither formed nor does it decompose when formed. Nakahara and Kikui [8], report the interference effect from 0.5 mg l^{-1} of Ni on the signal from 200 μg l^{-1} of Se (the interference/selenium ratio 2.5). Tao and Sturgeon [19] found no signal suppression for 500 μg l^{-1} of Se when 50 000 mg l^{-1} of Ni was present (the interference/selenium ratio 100 000). In this work, the selenium signal from 20 μg l^{-1} of Se without masking reagent remained constant up to a concentration of 600 mg l^{-1} (the interference/selenium ratio 30 000).

Nakahara and Kikui [8] report a 5 mg l^{-1} of Co tolerance limit for 200 μg l^{-1} of Se (the interference/selenium ratio 25). Tao and Sturgeon [19] studied the interference of Co, and found that 25 000 mg l^{-1} could be tolerated in a solution of 500 μg l^{-1} of Se without interference (the interference/selenium ratio 50 000). Our system reaches a concentration of 500 mg l^{-1} of Co without interference in a solution of 20 μg l^{-1} of Se (the interference/selenium ratio 25 000).

Interference reduction found may also arise as a consequence of the rapid gas/liquid separation of the analyte as postulated in Refs. [17,18,27].

The calibration curves obtained with both systems present in similar slopes, however, the detection limits ($3\sigma_b$) calculated between 1 and 15 μg l^{-1} are different. The detection limits (LOD) were 0.2 and 0.8 μg l^{-1} for DHGN with 70 and 120 μm, respectively. The difference found is because the emission signal obtained with the 120 μm DHGN is less reproducible than with the 70 μm DHGN. The reason for this is possibly due to the fact that the primary aerosol produced by the latter is finer and more homogeneous. Therefore, the hydride is generated in a more constant manner in time, producing a more reproducible signal. The detection limit found with 70 μm DHGN is substantially better than those reported for similar

Table 5
Results of the analysis of reference materials

Sample	Precision (% R.S.D.[a])	Certified value[b]	Found value[c]
Not-fat milk powder (NIST 1549) $\mu g\ g^{-1}$	7	0.11 ± 0.01	0.113 ± 0.008
Oyster tissue (NIST 1566 A) $\mu g\ g^{-1}$	3	2.21 ± 0.24	2.30 ± 0.06
Human urine (Urine metals control Lyphochek®) $\mu g\ l^{-1}$	7	67.0 ± 14	71.0 ± 5
	Reference value		
Sediments (IAEA/soil-7) $\mu g\ g^{-1}$	21	0.4 ± 0.2	0.43 ± 0.09

[a] Relative standard deviation of six replicate measurements.
[b] Mean and 95% confidence limits.
[c] Mean $\pm$ S.D. of six replicates.

systems based on the nebulizer modified for hydride production at very short reaction time and rapid separation of the gaseous products (0.5 [24], 6 [17] and 2 [18] $\mu g\ l^{-1}$). Detection limits of 0.3 [9], 0.45 [21], 0.6 [7,8], 0.8 [19], 1 [41], 3 [23] ng ml^{-1} for conventional systems of hydride generation by ICP–OES without preconcentration procedures have been reported in the literature. With this new hydride generator, LODs of the same order as the best reported with conventional hydride generation systems, but with a much simpler system can be reached. Additionally, there is no need to change the apparatus in order to work in normal mode with the ICP, since this system may be used for hydride forming elements and for those that do not form them.

The accuracy was also evaluated. The proposed methodology was applied to the determination of selenium in several certified reference materials and a standard reference material. Simple aqueous standards of 0.5–50 $\mu g\ l^{-1}$ Se(IV) in 2 M HCl were used for calibration. The results obtained are shown in Table 5. There is no significant difference at the 95% confidence level between the measured and certified values. The Relative standard deviation (R.S.D) for the selenium content in these certified materials was in the 2–7% range and 21% for the sediment (IAEA/soil-7) standard reference material.

4. Conclusions

This new direct hydride generation nebulizer (DHGN) system described has clear potential benefits over other commonly used HG systems in ICP OES in many aspects. It can be used for the determination of elements that produce volatile hydrides or as a conventional nebulizer or simultaneously for both. It produces a rapid response with low memory effect. It reduces the interference level of Ni, Co and Cu. It is a very economical hydride generation device with which detection limits of the same order as the best reported in HG–ICP OES are obtained without the need to make changes in the basic instrumentation of the ICP equipment. Detection limits of 0.2 $\mu g\ l^{-1}$ of selenium was found that was better than those reported for similar systems based on a modified nebulizer.

The response surface model used fits well to the experimental development. The 70 μm DHGN is better fitted to the model than the 120 μm DHGN. Linear effects are observed to prevail over the quadric effects. Development of the experimental design in blocks permitted better control of the ICP drift with respect to time. The selenium emission signal produced by the DHGN with a carrier gas orifice of 70 μm is more affected by all the factors under study compared to the DHGN with a carrier gas orifice of 120 μm. The 70 μm solution channel nebulizer exhibits a better detection limit and a lower interference level than the 120 μm nebulizer. The results show the importance of the primary aerosol quality on the response of the system, which constitutes the evidence that the hydride generation reaction is being carried out in the aerosol owing to droplet collisions between the reductant and sample solution.

Acknowledgments

The authors appreciate the help provided by Ivanka Cyitanich de Maslov in preparing the manuscript.

References

[1] J. Néve, Physiological and nutritional importance of selenium, Experientia 47 (1991) 187–193.
[2] K. Schwarz, Essentially and metabolic functions of selenium, Medl Clinics North America 60 (1976) 745–758.
[3] Handbook on the Toxicology of Metals in: Friberg L., Nordberg G.F., Vouk V.B. (Eds.), Specific metals, Vol. II, Elsevier, Amsterdam, 498–520.
[4] M. Sanz Alaejos, C. Díaz Romero, Analysis of selenium in body fluids: a review, Chem. Rev. 95 (1995) 227–257.
[5] A.D. Campbell, A critical survey of hydride generation techniques in atomic spectroscopy, Pure Appl. Chem. 64 (1992) 227–244.
[6] T. Wickstrøm, W Lund, R. Bye, Reduction of gaseous phase interference in hydride generation using inductively coupled plasma atomic emission instead of flame heated quartz tube atomic absorption spectrometry: determination of selenium in nickel alloys and low-alloy steels, J. Anal. At. Spectrom. 10 (1995) 809–813.
[7] Z. Mianzhi, R.M. Barnes, Determination of trace elements in serum using inductively coupled plasma atomic spectroscopy with hydride generation and chelating resin preconcentration, Appl. Spectrosc. 38 (1984) 635–644.
[8] T. Nakahara, N. Kikui, Determination of trace concentrations of selenium by continuous hydride generation-inductively coupled plasma atomic emission spectrometry, Spectrochim. Acta. Part B 40 (1985) 21–28.
[9] L.D. Martinez, E. Saidman, E. Marchevsky, R. Olsina, Determination of selenium in geochemical samples by flow injection hydride generation inductively coupled plasma atomic emission spectrometry following on-line removal of iron interference by anion exchange, J. Anal. At. Spectrom. 12 (1997) 487–489.
[10] J. Stripeikis, M. Tudino, O. Troccoli, R. Wuilloud, R. Olsina, L. Martínez, On-line copper and iron removal and selenium(VI) pre-reduction for the determination of total selenium by flow-injection hydride generation-inductively coupled plasma optical emission spectrometry, Spectrochim. Acta Part B 56 (2001) 93–100.
[11] A.E. Smith, Interferences in the determination of elements that form volatile hydrides with sodium borohydride using atomic-absorption spectrophotometry and the argon- hydrogen flame, Analyst 100 (1975) 300–306.
[12] G.F. Kirbright, M. Taddia, Application of masking agents in minimizing interferences from some metal ions in the determination of arsenic by atomic absorption spectrometry with hydride generation technique, Anal. Chim. Acta 100 (1978) 145–150.
[13] J. Agterdenbos, D. Bax, A study on the generation of hydrogen selenide and decomposition of tetrahydroborate in hydride-generation atomic absorption spectrometry, Anal. Chim. Acta 188 (1986) 127–135.
[14] T. Wichstrøm, W. Lund, R. Bye, Transport of nickel, cobalt, iron and chromium to the atom cell during a hydride generation process, Analyst 121 (1996) 201–204.
[15] P. Pohl, W. Zyrnicki, On the transport of some metals into inductively coupled plasma during hydride generation process, Anal. Chim. Acta 429 (2001) 135–143.
[16] E. Lugowska, I.D. Brindle, Potentiometric investigations of nickel, iron and cobalt interferences in the generation of selenium hydride by sodium tetrahydroborate, Analyst 122 (1997) 1559–1568.
[17] W.W. Ding, R.E. Sturgeon, Minimization of transition metal interferences with hydride generation techniques, Anal. Chem. 69 (1997) 527–531.
[18] G.H. Tao, R.E. Sturgeon, Sample nebulization for minimization of transition metal interferences with selenium hydride generation ICP–AES, Spectrochim. Acta Part B 54 (1999) 481–489.
[19] M. Thompson, B. Pahlavanpour, S.J. Walton, Simultaneous determination of trace concentrations of arsenic, antimony, bismuth, selenium and tellurium in aqueous solution by introduction of the gaseous hydrides into an inductively coupled plasma source for emission spectrometry, Analyst 103 (1978) 568–579.
[20] P.D. Goulden, D.H.J. Anthony, K.D. Austen, Determination of arsenic and selenium in water, fish and sediments by inductively coupled argon plasma emission spectrometry, Anal. Chem. 53 (1981) 2027–2029.
[21] J.D. Hwang, G.D. Guenther, J.P. Diomiguardi, Hydride generator system for a 1-Kw inductively coupled plasma, Anal. Chem. 61 (1989) 285–288.
[22] I.D. Brindle, H. Alarabi, S. Karshman, X. Le, S. Zheng, H. Chen, Combined generator/separator for continuous hydride generation application to on-line pre-reduction of arsenic(v) and determination of arsenic in water by emission spectrometry, Analyst 117 (1992) 407–411.
[23] C. Rigby, I.D. Brindle, Determination of arsenic, antimony, bismuth, germanium, tin, selenium and tellurium in 30% zinc sulfate solution by hydride generation inductively coupled plasma atomic emission spectrometry, J. Anal. At. Spectrom. 14 (1999) 253–258.
[24] K.A. Wolnik, F.L. Fricke, M.H. Hahn, J.A. Caruso, Sample introduction system for simultaneous determination of volatile elemental hydrides and other elements in foods by inductively coupled plasma atomic emission spectrometry, Anal. Chem. 53 (1981) 1030–1035.
[25] B. Huang, Z. Zhang, X. Zeng, A new nebulizer-hydride generator system for simultaneous multilelement inductively coupled plasma-atomic emission spectrometry, Spectrochim. Acta Part B 42 (1987) 129–137.

[26] Y. Feng, J. Cao, Simultaneous determination of arsenic(V) and arsenic(III) in water by inductively coupled plasma atomic emission spectrometry using reduction of arsenic(V) by L-cysteine and a small co-centric hydride generation without a gas liquid separator, Anal. Chim. Acta 293 (1994) 211–218.
[27] C. Moor, J.W.H. Lam, R.E. Sturgeon, A novel introduction system for hydride generation-inductively coupled plasma mass spectrometry: determination of selenium in biological materials, J. Anal. At. Spectrom. 15 (2000) 143–1479.
[28] D.O. Massart, B.G.M. Vandenginste, S.N. Deming, Y Michotte, L. Kaufman, Chemometrics; A Textbook, 1st ed, Elsevier, Amsterdan, 1988, pp. 59–74.
[29] B. Hilligsøe, E.H. Hansen, Application of factorial designs and simplex optimisation in the development of flow injection-hydride generation-graphite furnace atomic absorption spectrometry (FI-HG-GFAAS) procedures as demonstrated for the determination of trace levels of germanium, Fresenius J. Anal. Chem. 358 (1997) 775–780.
[30] X. Guo, X. Guo, Optimization of hydride generation atomic fluorescence spectrometry for the determination of trace amounts of germanium: emphasis on acidity and interferences, Anal. Chim. Acta 373 (1998) 303–310.
[31] A. Dreyer, E. Montiel, N. Coello, Utilización de la metodología de superficie de respuesta en la optimización de un medio de cultivo para la producción de L-lisina por *Corynebacterium glutamicum*, Agronomía Trop. 50 (2000) 167–188.
[32] J. Sanz, M. Pérz, M.T. Martínez, M. Plaza, Optimization of dimethyltin chloride determination by hydride generation gas phase molecular absorption spectrometry using a central composite design, Talanta 51 (2000) 849–862.
[33] P. Bermejo-Barrera, O. Muñiz-Naveiro, A. Moreda-Piñeiro, A. Bermejo-Barrera, The multivariate optimization of ultrasonic bath-induced acid leaching for the determination of trace elements in seafood products by atomic absorption spectrometry, Anal. Chim. Acta 439 (2001) 211–227.
[34] United Stated Enviromental Protection Agency (EPA), Method 3052, Microwave asisted acid digestion of siliceos and organical based matrices, 1996.
[35] Microwave sample preparation note, FD-14, CEM corporation. Printed USA, 1994.
[36] JMP. (ver 3.2.1). SAS Institute Inc. 1997.
[37] Design-Expert versión 6 software para Windows. 2001.
[38] Statistic made ease Mathematica for windows, Wolfram Research, 1997.
[39] A. Montaser, M.G. Minnich, J.A. McLean, H. Liu, J.A. Caruso, C.W. McLeod, in: A. Montaser (Ed.), Inductively Coupled Plasma Mass Spectrometry, Wiley-VCH, Inc, 1998, pp. 113–123, Chapter 3, ISBN 0-471-18620-1.
[40] A.I Khurry, J.A. Cornell, Response Surface, Marcell Dekker Inc, New York, 1966, p. 510.
[41] K.A. Anderson, B. Isaacs, Simultaneous determination of arsenic, selenium, and antimony in environmental samples by hydride generation for inductively coupled plasma atomic emission spectrometry, J. AOAC Int. 78 (1995) 1055–1060.